International Journal of Robust and Nonlinear Control

WILEY

RESEARCH ARTICLE OPEN ACCESS

Adaptive Sliding-Mode Control of a Perturbed Diffusion Process With Pointwise In-Domain Actuation

Paul Mayr[1] | Alessandro Pisano[2] | Stefan Koch[1] | Markus Reichhartinger[1]

[1]Institute of Automation and Control, Graz University of Technology, Graz, Austria | [2]Department of Electrical and Electronic Engineering, University of Cagliari, Cagliari, Italy

Correspondence: Paul Mayr (paul.mayr@tugraz.at)

Received: 30 June 2025 | **Revised:** 13 November 2025 | **Accepted:** 21 January 2026

Keywords: adaptive control | diffusion process | distributed parameter systems | robust control | sliding mode control

ABSTRACT

A sliding mode–based adaptive control law is proposed for a class of diffusion processes featuring a spatially-varying uncertain diffusivity and equipped with several point-wise actuators located at the two boundaries of the spatial domain as well as in its interior. The system is additionally perturbed by matched disturbances which are assumed to be uniformly bounded along with their time derivatives. The corresponding constant bounds are *unknown*, thus motivating the use of an adaptive control strategy. To achieve global asymptotic stability of the origin in the L_2-sense, a control law consisting of a proportional and discontinuous term is proposed. The gain of the discontinuous term is continuously adjusted according to a gradient-based adaptation algorithm. The stability and convergence analysis is Lyapunov-based and it constructively yields simple tuning conditions for the controller gain parameters. Simulation results are finally discussed to support the theoretical findings.

1 | Introduction

Control of dynamical systems for the purpose of stabilization or reference tracking often follows a model-based approach in which a mathematical model of the plant is exploited for feedback loop design. Most of the time, these mathematical models are characterized by a finite number of ordinary differential equations that approximate the behavior of the given system. While this approximation often suffices to effectively control real-world systems, there is also a substantial amount of processes where this finite-dimensional approximation falls short. Such processes appear in applications like, for example, lithium-ion batteries [1], flow reactors [2] or renewable energy systems [3]. What these systems have in common is their spatially-varying dynamical behavior, requiring models expressed in terms of Partial Differential Equations (PDEs).

A common way to affect the behaviour of distributed parameter systems is by means of actuators placed at the boundaries of the spatial domain, thus motivating the research field of boundary control. A powerful method for the boundary control of PDEs is the so-called *Backstepping* [4–7] in which the controller is designed via a state transformation such that the closed-loop system behaves like a chosen pre-specified target system. There are, however, also systems which are actuated inside of the spatial domain, hence, research is also concerned about extending the backstepping technique to PDEs with in-domain actuation [8].

A common goal in control design is the robustification of the closed loop against disturbances such as parametric uncertainties or external perturbations. The backstepping technique has been accordingly revisited, and *adaptive* backstepping boundary controllers have been developed to deal with parametric uncertainties [9–13]. A control method which is especially suited for suppressing external perturbation signals is the sliding-mode control technique, which renders the closed loop insensitive to matched disturbances, that is, disturbances entering on the dynamics in the same channel as the control input does. This is achieved by

https://doi.org/10.1002/rnc.70431

incorporating a discontinuity in the control law that can compensate for the disturbances which are assumed to be bounded in magnitude.

Sliding mode control has been successfully applied to distributed parameter systems as it is documented, for example, in References [14–16] or, more recently, in References [17, 18].

A popular class of distributed parameter systems considered in the sliding mode control literature is that of diffusion processes [17, 19–22]. They model a wide range of physical phenomena such as chemical diffusion or heat conduction. In the latter case of thermal control applications, Neumann actuation using current-controlled thermoelectric devices is an attractive option due to their fast response, which is beneficial for rapidly changing temperature profiles or compensation of fluctuating external disturbances. Therefore, sliding mode control is a well suited technique which takes full advantage of the high available control bandwidth which is typical for such current control loops.

As such inner control loops can induce uncertain actuator dynamics, remarkably, uncertain first-order actuator dynamics were included in the process model in Reference [23]. Although in the sliding mode control setting the insertion of actuator dynamics usually causes chattering, in Reference [23] a control law comprising a linear PD term and a discontinuous relay term was proposed capable of guaranteeing exponential stability of the closed-loop solutions.

It is typically assumed that bounds of the disturbance—either on itself or on its time derivative—are known such that the tuning parameters of the control law can be adjusted accordingly. However, when no such bounds are known, one has to resort to *adaptive* strategies that update the control parameters online and therefore avoid crude overestimation of the tuning gains. Utilizing gains that are not unnecessarily large is an important aspect in sliding mode control as it helps to reduce chattering phenomena. Adaptive algorithms of this kind are presented in References [24, 25] and applications to distributed parameter systems are found in References [26–28]. It should be noted that bidirectional adaptation algorithms, where the adaptive control gain can both increase and decrease, are considered in References [25, 27, 28], whereas monodirectional gradient-based algorithms are considered in References [24, 26] and in the present paper. Although bidirectional algorithms appear to possess more desirable properties of chattering alleviation, they exhibit, however, weaker convergence features in that only the attainment of practical stability, for example, a bounded vicinity of the origin, can be guaranteed. In contrast, the monodirectional gradient based adaptation algorithms considered in the present paper, allow asymptotic stability properties to be proven.

The transition from the boundary control scenario to the combined boundary/in-domain actuation is relevant as it allows to exert control actions in the interior of the spatial domain to cope with, for example, local instabilities or in-domain disturbances. Indeed, distributed control is hardly implementable in practice, and the usage of several in-domain collocated actuators represents a viable alternative to distributed control. Dealing with collocated in-domain actuation, however, raises considerable theoretical challenges of proving closed-loop stability. These challenges are overcome, in the present paper, by exploiting the idea of partitioning the whole system into smaller coupled susbystems, defined on subsets of the overall spatial domain, and modeled by PDEs with boundary control only (an idea brought up in Reference [8] and suitably reshaped in the present work).

Motivated by the above considerations, in the present paper the stabilization of an uncertain diffusion process equipped with both boundary and in-domain point-wise actuators and additionally subject to external matched disturbances is considered. The unknown disturbances and their time derivatives are both assumed to be uniformly bounded, however, the corresponding bounds are *unknown*. An adaptive sliding-mode based control strategy is therefore employed with a gradient-based adaptation algorithm adjusting the magnitude of the relay control term. It allows the gains to increase until insensitivity against the disturbances is achieved and asymptotic convergence to zero in the L_2-sense is guaranteed.

A similar scenario is considered in Reference [26] where the adaptive sliding-mode based control algorithm is applied via a unique actuator/sensor pair located at the *boundary* of the spatial domain. Furthermore, in Reference [29] adaptive unit-vector control is applied to the diffusion process via a *distributed* control input. The present paper fills the gap by considering *point-wise in-domain* actuation. The same adaptive control algorithm employed in Reference [26] is applied at each actuation point, asymptotically rejecting possibly present matched disturbances.

A proof for the global asymptotic stability of the origin in the L_2-sense is given via a Lyapunov-based stability analysis. This is enabled by a preliminary investigation in which the considered system is split up at the N actuation points into $N-1$ coupled subsystems with boundary control only. This partitioning procedure is necessary to demonstrate the claimed stability features since the Lyapunov analysis adopted in References [20, 26] fail to generalize directly to the adaptive and in-domain actuation setting dealt with in the present paper. Note that, instead of dealing with these subsystems individually, the coupling requires the construction of combined Lyapunov functions that take into account the entire system.

This article is structured as follows: Section 2 introduces the considered system and states the control problem at hand. Section 3 describes the employed control and adaptation laws which is followed by an investigation in which the overall system is split into subsystems. The obtained stability result is summarized in a theorem and proven by a Lyapunov-based convergence analysis. Simulation results are presented in Section 4 and concluding remarks are given in Section 5.

1.1 | Notation

The notation used throughout the paper is fairly standard. $H^{\ell}(a,b)$, with $a<b$ and $\ell = 0,1,2,\ldots$, denotes the Sobolev space of scalar functions $f(\zeta)$ on $[a,b]$ with square integrable derivatives $f^{(i)}(\zeta)$ up to the order ℓ and the H^{ℓ}-norm

$$\|f(\cdot)\|_{H^{\ell}(a,b)} = \sqrt{\int_a^b \sum_{i=0}^{\ell} [f^{(i)}(\zeta)]^2 \, \mathrm{d}\zeta}. \tag{1}$$

We shall also utilize the standard notations $H^0(a,b) = L_2(a,b)$ and $\|f(\cdot)\|_{H^0(a,b)} = \|f(\cdot)\|_{L_2(a,b)}$. Partial derivatives are indicated by indices, that is,

$$z_t(x,t) = \frac{\partial z(x,t)}{\partial t}, \quad z_x(x,t) = \frac{\partial z(x,t)}{\partial x}, \quad z_{xx}(x,t) = \frac{\partial^2 z(x,t)}{\partial x} \tag{2}$$

whereas total time derivatives are denoted as

$$\dot{V}(h(t)) = \frac{\mathrm{d}V(h(t))}{\mathrm{d}t}. \tag{3}$$

Derivatives of functions depending on a scalar spatial variable only are indicated by

$$\varphi'(x) = \frac{\mathrm{d}\varphi(x)}{\mathrm{d}x}. \tag{4}$$

$sign(\cdot)$ denotes the multi-valued function[1] $sign(\sigma) : \mathbb{R} \to [-1,1]$ such that

$$sign(\sigma) \in \begin{cases} \{1\} & \text{for } \sigma > 0 \\ [-1,1] & \text{for } \sigma = 0 \\ \{-1\} & \text{for } \sigma < 0 \end{cases}. \tag{5}$$

2 | Problem Formulation

Consider the space- and time-varying scalar field $z(x,t)$, evolving in the space $L_2(0,1)$, with the spatial variable $x \in [0,1]$ and time variable $t \geq 0$. Let it be governed by the perturbed boundary value problem (BVP) given by the partial differential equation (PDE)

$$z_t(x,t) = \left[\theta(x) z_x(x,t)\right]_x + \sum_{i=2}^{N-1} \theta(x_i)\delta(x - x_i)\left[u_i(t) + \psi_i(t)\right] \tag{6}$$

with Neumann-type boundary conditions

$$z_x(0,t) = -\left[u_1(t) + \psi_1(t)\right], \tag{7a}$$

$$z_x(1,t) = u_N(t) + \psi_N(t). \tag{7b}$$

The system is initialized with the initial condition

$$z(x,0) = z_0(x) \in L_2(0,1). \tag{8}$$

Function $\theta(x)$ represents the spatially-varying diffusion coefficient. The manipulable control inputs are the signals $u_i(t)$ ($i = 1,2,\ldots,N$), and the corresponding actuator spatial locations respectively coincide with the points $x_i \in [0,1]$, where $0 = x_1 < x_2 < \ldots < x_N = 1$. Therefore, the manipulable control signals can be divided into two groups: the boundary inputs $u_1(t)$ and $u_N(t)$, affecting the BVP through the BCs (7a) and (7b), and the remaining in-domain control inputs $u_2(t), u_3(t), \ldots, u_{N-1}(t)$ featuring the input shape functions $\theta(x_i)\delta(x - x_i)$, where $\delta(\cdot)$ stands for the Dirac delta function. The considered BVP is also subject to the matched disturbances $\psi_i(t)$, $i = 1,2,\ldots,N$.

It is assumed that the only available measurements consist of the collocated states $z(x_i,t)$ with $i = 1,2,\ldots,N$.

The class of admissible disturbances is specified in the following Assumption.

Assumption 1. The disturbances $\psi_i(t)$ and their time derivatives are of class $L_\infty(0,\infty)$ and there exist unknown constants Φ_i and $\Phi_{\mathrm{d},i}$ such that the next relations hold $\forall i = 1,2,\ldots,N$ and $\forall t \geq 0$:

$$|\psi_i(t)| \leq \Phi_i, \tag{9}$$

$$|\dot{\psi}_i(t)| \leq \Phi_{\mathrm{d},i} \tag{10}$$

Since the constants Φ_i and $\Phi_{\mathrm{d},i}$ involved in the inequalities (9) and (10) are supposed to be unknown, an adaptive and robust control strategy is needed in order to achieve disturbance rejection.

The uncertain spatially-varying diffusivity $\theta(x)$ is required to fulfill the requirements specified in the next Assumption.

Assumption 2. The uncertain spatially-varying diffusivity $\theta(x)$ is of class $C^1(0,1)$ and there exist unknown constants θ_{m} and θ_{M} such that

$$0 < \theta_{\mathrm{m}} \leq \theta(x) \leq \theta_{\mathrm{M}} \quad \forall x \in [0,1]. \tag{11}$$

The control goal is to design suitable control signals $u_i = u_i(z(x_i,t))$ capable of guaranteeing closed-loop asymptotic stability in the L_2-sense despite the presence of parameter uncertainties and external perturbations in the BVP (6) and (7b) to be controlled. The next section proposes a possible solution relying on the adaptive sliding-mode control design method.

3 | Controller Synthesis

The control laws

$$u_i(t) = -k_i z(x_i,t) - M_i(t) sign\big(z(x_i,t)\big), \quad i = 1,\ldots,N \tag{12}$$

comprising proportional terms and discontinuous relay terms with adaptive magnitudes are proposed. The time-varying adaptive magnitude $M_i(t)$ of the discontinuous terms are adjusted according to the adaptation laws

$$\dot{M}_i(t) = \gamma_i |z(x_i,t)|, \quad i = 1,\ldots,N \tag{13}$$

$$M_i(0) = M_{0,i} \tag{14}$$

where the initial values $M_{0,i}$ satisfy

$$M_{0,i} \geq 0, \quad i = 1,\ldots,N. \tag{15}$$

Note that (12) and (13) describe *individual* controllers, that is, there is no coupling between them.

With positive adaptation parameters

$$\gamma_i > 0, \quad i = 1,\ldots,N \tag{16}$$

the right-hand side of (13) is non-negative hence (13) to (16) describe a *monodirectional* adaptation law, that is, the gains $M_i(t)$ are monotonically increasing. More precisely, the gain $M_i(t)$ increases during the transient until it is large enough to dominate the magnitude of the disturbance $\psi_i(t)$.

Tuning the controllers requires the choice of the initial values $M_{0,i}$, the adaptation gains γ_i, and the proportional gains k_i. Although $M_{0,i}$ and γ_i can arbitrarily be chosen in accordance with (15) and (16), the proportional gains are required to satisfy the more involved inequalities

$$k_i \geq \gamma_i, \quad \forall i \in \{0, \ldots, N\}, \tag{17}$$

$$\max_{i\in\{1,\ldots,N\}} \{k_i\} \geq \frac{1}{2}. \tag{18}$$

The stability and convergence proof to be developed will provide a constructive derivation of the above tuning inequalities (15) to (18) and will additionally formally demonstrate that the gains $M_i(t)$ are uniformly bounded in the closed-loop system.

3.1 | Well-Posedness of the Closed-Loop System

The solution of the BVP (6), (7a) and (7b) beyond the discontinuity manifolds $z(x_i, t) = 0$ is adopted in the weak sense according to the next Definiton (see also Definition 1 of Reference [20] for a related result)

Definition 1. A continuous function $\tilde{z}(\cdot, t) \in H^1(0, 1)$ satisfying the boundary conditions (7a) and (7b) is said to be a weak solution of the BVP (6), (7a) and (7b) on $[0, \tau)$ if for every $\tilde{\varphi}(x) \in H^1(0, 1)$ the function $\int_0^1 \tilde{z}(x, t)\tilde{\varphi}(x)\,\mathrm{d}x$ is absolutely continuous on $[0, \tau)$ and the relation

$$\int_0^1 \tilde{z}_t(x, t)\tilde{\varphi}(x)\,\mathrm{d}x = -\int_0^1 \theta(x)\tilde{z}_x(x, t)\tilde{\varphi}'(x)\,\mathrm{d}x + \sum_{i=1}^{N} \theta(x_i)\left[u_i(t) + \psi_i(t)\right]\tilde{\varphi}(x_i) \tag{19}$$

holds for almost all $t \in [0, \tau)$.

The weak formulation (19) is obtained by multiplying the PDE (6) by a test function $\tilde{\varphi}(x)$, integrating over the spatial domain $x \in (0, 1)$, applying integration by parts and considering boundary conditions (7a) and (7b). It is made use of the well-known property

$$\int_0^1 \delta(x - x_i)\tilde{\varphi}(x)\,\mathrm{d}x = \tilde{\varphi}(x_i) \tag{20}$$

of the Dirac delta function and the weak derivative $\tilde{\varphi}'(x)$ of $\tilde{\varphi}(x)$.

Solutions *on* discontinuity manifolds are adopted in the Filippov sense. Well-posedness of the closed-loop solutions in a more involved BVP equipped with pointwise in-domain and boundary actuators, like in the present case, but featuring additional reaction and advection terms was already analyzed in Reference [20] under proportional-plus-relay control laws similar to (12) but of non-adaptive nature (i.e., with $M(t) = M^* = \text{const.}$). Furthermore, well-posedness of a similar diffusion PDE as that investigated in the present paper, but equipped with a unique scalar boundary control is addressed in Reference [26] under a proportional-plus-relay adaptive control law identical to (12) to (16). Hence, the interested reader is referred to these two articles and additionally for more details on weak and Filippov solution notions and well-posedness results in the setting of parabolic PDEs with discontinuous point-wise in-domain and/or boundary feedback control inputs.

3.2 | Division Into Coupled Subsystems With Boundary Actuation

In order to handle the in-domain actuation of (6), the upcoming stability results of Section 3.3 rely on the idea of splitting the overall system into several coupled subsystems with boundary actuation only. This procedure is implemented by dividing the spatial domain $x \in [0, 1]$ into a number of subdomains whose boundaries are the actuation points x_i, and then deriving from the overall system dynamics the suitable BVP governing the solution in these sub-domains. Hence, in this section, a preliminary result is developed, which is then used in the stability analysis presented in Section 3.3. The idea of handling pointwise in-domain actuation by splitting the system at the actuation points is already brought up in Reference [8]. Here, this idea is extended and its validity is shown mathematically.

By splitting the system at the N actuation points x_i, $N - 1$ coupled subsystems characterized by the states $z_i(x, t)$ and defined into the spatial domains $x \in X_i \equiv (x_i, x_{i+1})$ are obtained, as it is visualized in Figure 1.

The states $z_i(x, t)$ evolve according to the BVPs given by the PDEs

$$z_{i,t}(x, t) = \left[\theta(x)z_{i,x}(x, t)\right]_x, \quad x \in (x_i, x_{i+1}), \quad i = 1, \ldots, N - 1 \tag{21}$$

with boundary conditions

$$z_{i,x}(x_i, t) = z_{i-1,x}(x_i, t) - \left[u_i(t) + \psi_i(t)\right], \tag{22a}$$

$$z_{i,x}(x_{i+1}, t) = z_{i+1,x}(x_{i+1}, t) + u_{i+1}(t) + \psi_{i+1}(t). \tag{22b}$$

For the description (21), (22a) and (22b) to be valid for the "boundary systems" $i = 1$ and $i = N - 1$, the definitions

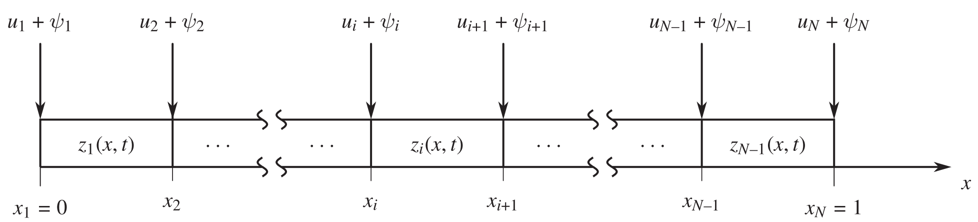

FIGURE 1 | For the purpose of analysis, the system is split at the actuation points into multiple subsystems with boundary actuation only. This allows incorporating the in-domain actuation into the Lyapunov analysis by boundary terms emerging from integration by parts.

$$z_{0,x}(x_1,t)=0, \tag{23a}$$

$$z_{N,x}(x_N,t)=0 \tag{23b}$$

are made. Note that the coupling between the subsystems occurs through the boundary conditions (22a) and (22b). The additional compatibility conditions

$$z_{i-1}(x_i,t)=z_i(x_i,t) \quad \forall i\in\{2,\dots,N-1\} \tag{24}$$

are also in force due to the fact that $z(\cdot,t)$ is continuous by Definition 1.

In the following we relate the weak solutions of the subsystems (21), (22a), and (22b) to the weak solution of the overall system (6), (7a), and (7b) given in Definition 1.

Definition 2. A continuous function $z_i(\cdot,t)\in H^1(x_i,x_{i+1})$ satisfying the boundary conditions (22a) and (22b) is said to be a weak solution of the BVP (21), (22a) and (22b) on $[0,\tau)$ if for every $\varphi_i(x)\in H^1(x_i,x_{i+1})$ the function $\int_{x_i}^{x_{i+1}} z_i(x,t)\varphi_i(x)\,\mathrm{d}x$ is absolutely continuous on $[0,\tau)$ and the relation

$$\begin{aligned}\int_{x_i}^{x_{i+1}} z_{i,t}(x,t)\varphi_i(x)\,\mathrm{d}x &= \theta(x_{i+1})z_{i+1,x}(x_{i+1},t)\varphi_i(x_{i+1})\\ &\quad+\theta(x_{i+1})\left[u_{i+1}(t)+\psi_{i+1}(t)\right]\varphi_i(x_{i+1})\\ &\quad-\theta(x_i)z_{i-1,x}(x_i,t)\varphi_i(x_i)\\ &\quad+\theta(x_i)\left[u_i(t)+\psi_i(t)\right]\varphi_i(x_i)\\ &\quad-\int_{x_i}^{x_{i+1}}\theta(x)z_{i,x}(x,t)\varphi_i'(x)\,\mathrm{d}x\end{aligned} \tag{25}$$

holds for almost all $t\in[0,\tau)$.

As in Definition 1, the weak solution definition (25) is obtained by multiplying the PDE (21) with a test function $\varphi_i(x)$, integrating over the spatial domain $x\in(x_i,x_{i+1})$ and applying integration by parts to the term

$$\begin{aligned}\int_{x_i}^{x_{i+1}}\left[\theta(x)z_{i,x}(x,t)\right]_x\varphi_i(x)\,\mathrm{d}x &= \theta(x)z_{i,x}(x,t)\varphi_i(x)\Big|_{x_i}^{x_{i+1}}\\ &\quad-\int_{x_i}^{x_{i+1}}\theta(x)z_{i,x}(x,t)\varphi_i'(x)\,\mathrm{d}x.\end{aligned} \tag{26}$$

Inserting boundary conditions (22a) and (22b) into (26) yields (25). Similar to (24) it is also required that

$$\varphi_i(x_{i+1})=\varphi_{i+1}(x_{i+1}) \quad \forall i\in\{1,\dots,N-2\} \tag{27}$$

to obtain continuous test functions.

Note that Definitions 1 and 2 can be combined into one general definition of a weak solution. Indeed, Definition 1 is obtained from Definition 2 for the special case $N=2$, $x_i=x_1=0$, $x_{i+1}=x_N=1$ and considering (23a) and (23b) in (25) together with (27).

We are now in a position to relate the weak solutions of the individual subsystems to the weak solution of the overall system in the following lemma.

Lemma 1. *Consider the weak solution $\tilde{z}(\cdot,t)$ of (6), (7a) and (7b) according to Definition 1. Then, $\tilde{z}(\cdot,t)$ coincides with*

$$z(\cdot,t)=\begin{cases} z_i(\cdot,t) & \text{for } x_i\le x<x_{i+1}\\ z_{N-1}(\cdot,t) & \text{for } x_{N-1}\le x\le x_N\end{cases} \tag{28}$$

where $z_i(\cdot,t)$, $i=1,\dots,N-1$ are the weak solutions of (21), (22a), (22b), (23a), (23b) and (24) according to Definition 2.

Proof. From (22b), (25) and (27) it is obtained that

$$\begin{aligned}\int_{x_i}^{x_{i+1}} z_{i,t}(x,t)\varphi_i(x)\,\mathrm{d}x &= \kappa_{i+1}-\kappa_i\\ &\quad+\theta(x_i)\left[u_i(t)+\psi_i(t)\right]\varphi_i(x_i)\\ &\quad-\int_{x_i}^{x_{i+1}}\theta(x)z_{i,x}(x,t)\varphi_i'(x)\,\mathrm{d}x\end{aligned} \tag{29}$$

where the variable

$$\kappa_i(t):=\theta(x_i)z_{i-1,x}(x_i,t)\varphi_i(x_i) \tag{30}$$

is introduced for brevity. The strategy followed now is computing the sum of (29) over all intervals (x_i,x_{i+1}), $i=1,\dots,N-1$, to recover the weak form (19) of the overall system (6), (7a) and (7b). To that end, consider the sum

$$\sum_{i=1}^{N-1}\left[-\kappa_i(t)+\kappa_{i+1}(t)\right]=-\kappa_1(t)+\kappa_N(t) \tag{31}$$

Due to (22b), (23a) and (23b) functions $\kappa_1(t)$ and $\kappa_N(t)$ are given by

$$\kappa_1(t)=\theta(x_1)z_{0,x}(x_1,t)\varphi_1(x_1)=0, \tag{32}$$

$$\begin{aligned}\kappa_N(t)&=\theta(x_N)z_{N-1,x}(x_N,t)\varphi_N(x_N)\\ &=\theta(x_N)\left[u_N(t)+\psi_N(t)\right]\varphi_N(x_N).\end{aligned} \tag{33}$$

Computing the sum over (29) and considering (31) and (33) yields

$$\begin{aligned}\sum_{i=1}^{N-1}\int_{x_i}^{x_{i+1}} z_{i,t}(x,t)\varphi_i(x)\,\mathrm{d}x &= \sum_{i=1}^{N}\theta(x_i)\left[u_i(t)+\psi_i(t)\right]\varphi_i(x_i)\\ &\quad-\sum_{i=1}^{N-1}\int_{x_i}^{x_{i+1}}\theta(x)z_{i,x}(x,t)\varphi_i'(x)\,\mathrm{d}x.\end{aligned} \tag{34}$$

With (28) and

$$\varphi(x):=\begin{cases}\varphi_i(x) & \text{for } x_i\le x<x_{i+1}\\ \varphi_{N-1}(x) & \text{for } x_{N-1}\le x\le x_N\end{cases} \tag{35}$$

it is therefore obtained that

$$\begin{aligned}\int_0^1 z(x,t)\varphi(x)\,\mathrm{d}x &= \sum_{i=1}^{N}\theta(x_i)\left[u_i(t)+\psi_i(t)\right]\varphi(x_i)\\ &\quad-\int_0^1\theta(x)z_x(x,t)\varphi'(x)\,\mathrm{d}x\end{aligned} \tag{36}$$

which is equivalent to the weak form (19). □

3.3 | Stability Analysis

A preliminary result is developed in the following Lemma and its proof. It presents a modification to the Poincaré inequality (see Reference [9]) where the L_2-norm of a function is estimated by the L_2-norm of its derivative and the function value at one of the boundaries of the spatial domain. It is desired to develop a similar inequality where the boundary term is replaced by the function evaluated at an arbitrary point of its domain. This inequality is derived in the following Lemma, and it is going to be used in the subsequent stability analysis.

Lemma 2. *For any $f \in H^1(0,1)$ and $0 \le x_0 \le 1$ it holds that*

$$\|f\|^2_{L_2(0,1)} \le 2f^2(x_0) + 4\|f'\|^2_{L_2(0,1)}. \tag{37}$$

Proof. The starting point for the proof are the conventional Poincaré inequalities given by

$$\|f\|^2_{L_2(0,1)} \le 2f^2(0) + 4\|f'\|_{L_2(0,1)}, \tag{38a}$$

$$\|f\|^2_{L_2(0,1)} \le 2f^2(1) + 4\|f'\|_{L_2(0,1)} \tag{38b}$$

(see Reference [9]). In a first step the inequalities (38a) and (38b) are transformed to work in the space $H^1(a,b)$ with an arbitrary interval $0 \le a < b \le 1$. To this end, consider the substitution

$$\xi = (b-a)x + a \tag{39}$$

such that $x = 0$ is mapped to $\xi = a$ and $x = 1$ to $\xi = b$. By introducing $\tilde{f}(\xi) = f(x)$ it is obtained via the chain rule that

$$f'(x) = \frac{\mathrm{d}f(x)}{\mathrm{d}x} = \frac{\mathrm{d}\tilde{f}(\xi(x))}{\mathrm{d}x} = \frac{\mathrm{d}\tilde{f}(\xi)}{\mathrm{d}\xi}\frac{\mathrm{d}\xi}{\mathrm{d}x} = \tilde{f}(\xi)(b-a). \tag{40}$$

Applying substitution (39) and (40) to (38a) in its integral form yields

$$\frac{1}{b-a}\int_a^b \tilde{f}^2(\xi)\,\mathrm{d}\xi \le 2\tilde{f}^2(a) + 4\frac{1}{b-a}\int_a^b [\tilde{f}(\xi)(b-a)]^2\,\mathrm{d}\xi \tag{41}$$

which is rewritten as

$$\|\tilde{f}\|^2_{L_2(a,b)} \le 2(b-a)\tilde{f}^2(a) + 4(b-a)^2\|\tilde{f}'\|^2_{L_2(a,b)}. \tag{42}$$

With (38b) it is similarly obtained that

$$\|\tilde{f}\|^2_{L_2(a,b)} \le 2(b-a)\tilde{f}^2(b) + 4(b-a)^2\|\tilde{f}'\|^2_{L_2(a,b)}. \tag{43}$$

By decomposing the norm $\|f\|^2_{L_2(0,1)}$ and applying (43) with $a = 0, b = x_0$ and (42) with $a = x_0, b = 1$ results in

$$\begin{aligned}\|f\|^2_{L_2(0,1)} &= \|f\|^2_{L_2(0,x_0)} + \|f\|^2_{L_2(x_0,1)} \\ &\le 2x_0 f^2(x_0) + 4x_0^2\|f'\|^2_{L_2(0,x_0)} \\ &\quad + 2(1-x_0)f^2(x_0) + 4(1-x_0)^2\|f'\|^2_{L_2(x_0,1)} \\ &= 2f^2(x_0) + 4x_0^2\|f'\|^2_{L_2(0,x_0)} \\ &\quad + 4(1-x_0)^2\|f'\|^2_{L_2(x_0,1)}. \end{aligned} \tag{44}$$

With $0 \le x_0^2 \le 1$ as well as $0 \le 1 - x_0^2 \le 1$ and recombining the norms $\|f'\|^2_{L_2(0,x_0)} + \|f'\|^2_{L_2(x_0,1)} = \|f'\|^2_{L_2(0,1)}$, inequality (37) is proven. □

The following theorem presents the result of the Lyapunov-based convergence analysis of the closed-loop system.

Theorem 1. *Consider PDE (6) with boundary conditions (7a) and (7b), initial condition (8), and let Assumptions 1and 2 be fulfilled. Let the system be controlled by the adaptive control laws (12) to (14) and let the control parameters be tuned according to (15) to (18). Then, the zero solution $z^*(x,t) = 0$ is globally asymptotically stable in the $L_2(0,1)$-sense, that is,*

$$\lim_{t\to\infty}\|z(\cdot,t) - z^*(\cdot,t)\|_{L_2(0,1)} = 0 \quad \forall z_0(x). \tag{45}$$

Proof. The structure of the proof is divided into four logical steps. In Step 1, it is preliminarily shown by Lyapunov analysis that the L_2-norm $\|z(\cdot,t)\|_{L_2(0,1)}$ of the potential closed-loop trajectories and the adaptive switching gains $M_i(t)$ are both uniformly bounded. In Step 2, by relying on the uniform boundedness properties proven in Step 1, the system is shown to be forward complete in the sense that its solutions globally exist for all $t \ge 0$. A more elaborated Lyapunov analysis is subsequently developed in Step 3 to show the uniform boundedness of $\int_0^1 \theta(x)z_x^2(x,t)\,\mathrm{d}x$ and $|z(x_i,t)|$, $i \in \{1,\dots,N\}$.

Finally, in Step 4 we further develop the Lyapunov analysis, eventually enabling the application of *Barbalat's* Lemma [30] to demonstrate the global asymptotic closed-loop stability in the L_2-sense.

Step 1: Uniform boundedness of $\|z(\cdot,t)\|_{L_2(0,1)}$ and $M_i(t)$

For the closed-loop system in question, consider the Lyapunov candidate function

$$V(t) = V_1(t) + V_2(t), \tag{46}$$

where

$$V_1(t) = \frac{1}{2}\|z(\cdot,t)\|^2_{L_2(0,1)} \tag{47}$$

and

$$V_2(t) = \frac{1}{2}\sum_{i=1}^{N}\frac{\theta(x_i)}{\gamma_i}\big(M_i(t) - \Phi_i\big)^2. \tag{48}$$

Strictly speaking $V_1(t)$ is a functional but for simplicity it is referred to as a function. Furthermore, $V_1(z(\cdot,t)) = V_1(t)$ is written for this, and, analogously for other functions.

The norm $\|z(\cdot,t)\|^2_{L_2(0,1)}$ in (47) is decomposed, thus giving

$$V_1(t) = \frac{1}{2}\sum_{i=1}^{N-1}\|z(\cdot,t)\|^2_{L_2(x_i,x_{i+1})} = \frac{1}{2}\sum_{i=1}^{N-1}\int_{x_i}^{x_{i+1}} z_i^2(x,t)\,\mathrm{d}x \tag{49}$$

where $z_i(x,t)$ are the weak solutions of the subsystems (21), (22a) and (22b). Computing the time derivative of (49) along potential weak solutions beyond the discontinuity manifolds $z(x_i, t) = 0$ by considering (21) and performing integration by parts yields

$$\begin{aligned}\dot{V}_1(t) &= \sum_{i=1}^{N-1} \int_{x_i}^{x_{i+1}} z_i(x,t) z_{i,t}(x,t)\,\mathrm{d}x \\ &= \sum_{i=1}^{N-1} \int_{x_i}^{x_{i+1}} z_i(x,t)\left[\theta(x) z_{i,x}(x,t)\right]_x\,\mathrm{d}x \\ &= \sum_{i=1}^{N-1}\left[\theta(x) z_{i,x}(x,t) z_i(x,t)\Big|_{x_i}^{x_{i+1}} - \int_{x_i}^{x_{i+1}} \theta(x) z_{i,x}^2(x,t)\,\mathrm{d}x\right].\end{aligned} \tag{50}$$

With (28) in mind, the integral terms in (50) are combined to obtain

$$\begin{aligned}\dot{V}_1(t) &= -\int_0^1 \theta(x) z_x^2(x,t)\,\mathrm{d}x + \sum_{i=1}^{N-1} \theta(x) z_{i,x}(x,t) z_i(x,t)\Big|_{x_i}^{x_{i+1}} \\ &= -\int_0^1 \theta(x) z_x^2(x,t)\,\mathrm{d}x + \sum_{i=1}^{N-1}\big[\theta(x_{i+1}) z_{i,x}(x_{i+1},t) \\ &\quad z_i(x_{i+1},t) - \theta(x_i) z_{i,x}(x_i,t) z_i(x_i,t)\big].\end{aligned} \tag{51}$$

Replacing into (51) the compatibility conditions (22a) and (24) under consideration of (28) yields

$$\begin{aligned}\dot{V}_1(t) = -\int_0^1 \theta(x) z_x^2(x,t)\,\mathrm{d}x + \sum_{i=1}^{N-1}\Bigg[&\underbrace{\theta(x_{i+1}) z_{i,x}(x_{i+1},t) z(x_{i+1},t)}_{\chi_{i+1}(t)} \\ &\underbrace{-\theta(x_i) z_{i-1,x}(x_i,t) z(x_i,t)}_{\chi_i(t)} + \theta(x_i)\left[u_i(t) + \psi_i(t)\right] z(x_i,t)\Bigg].\end{aligned} \tag{52}$$

Note that, similar to expression (29), also in (52) a term

$$\chi_i(t) = \theta(x_i) z_{i-1,x}(x_i,t) z(x_i,t) \tag{53}$$

along with its index-shifted version $\chi_{i+1}(t)$ appears. Exploiting similar manipulations as those made in (31), equation (52) is therefore simplified to

$$\begin{aligned}\dot{V}_1(t) &= -\int_0^1 \theta(x) z_x^2(x,t)\,\mathrm{d}x - \chi_1(t) + \chi_N(t) \\ &\quad + \sum_{i=1}^{N-1} \theta(x_i)\left[u_i(t) + \psi_i(t)\right] z(x_i,t).\end{aligned} \tag{54}$$

Due to (7b), (23a) and (28), the expressions $\chi_i(t)$ in (53) for $i = 1$ and $i = N$ evaluate to

$$\chi_1(t) = \theta(x_1) z_{0,x}(x_1,t) z(x_1,t) = 0, \tag{55}$$

$$\chi_N(t) = \theta(x_N) z_x(x_N,t) z(x_N,t) = \theta(x_N)\left[u_N(t) + \psi_N(t)\right] z(x_N,t). \tag{56}$$

Considering (55) and (56) in (54) results in

$$\dot{V}_1(t) = -\int_0^1 \theta(x) z_x^2(x,t)\,\mathrm{d}x + \sum_{i=1}^{N} \theta(x_i)\left[u_i(t) + \psi_i(t)\right] z(x_i,t) \tag{57}$$

By inserting in (57) the control laws (12) one finally arrives at

$$\begin{aligned}\dot{V}_1(t) &= -\int_0^1 \theta(x) z_x^2(x,t)\,\mathrm{d}x \\ &\quad - \sum_{i=1}^{N}\big[\theta(x_i) k_i z^2(x_i,t) + \theta(x_i) M_i(t) |z(x_i,t)| \\ &\quad - \theta(x_i)\psi_i(t) z(x_i,t)\big]\end{aligned} \tag{58}$$

Note that the discontinuous and multi-valued terms $sign\left(z(x_i,t)\right)$ enter $\dot{V}_1(t)$ via replacing the control laws (12) in (57). The existence of $\dot{V}_1(t)$ along the discontinuity manifolds $z(x_i,t) = 0$ and its single-valued nature are, however, still verified since the discontinuous terms feature the common multiplier $z(x_i,t)$ which is vanishing along the discontinuity manifold thereby making globally valid the expression (58) both beyond and along the discontinuity manifolds $z(x_i,t) = 0$.

The time derivative of $V_2(t)$ is derived by considering the adaptation law (13) and evaluates to

$$\dot{V}_2(t) = \sum_{i=1}^{N}\left[\theta(x_i) M_i(t) |z(x_i,t)| - \theta(x_i)\Phi_i |z(x_i,t)|\right]. \tag{59}$$

Combining (58) and (59) and taking advantage of (9) yields

$$\begin{aligned}\dot{V}(t) &= \dot{V}_1(t) + \dot{V}_2(t) \\ &= -\int_0^1 \theta(x) z_x^2(x,t)\,\mathrm{d}x + \sum_{i=1}^{N}\big[-\theta(x_i) k_i z^2(x_i,t) \\ &\quad + \theta(x_i)\psi_i(t) z(x_i,t) - \theta(x_i)\Phi_i |z(x_i,t)|\big] \\ &\leq -\int_0^1 \theta(x) z_x^2(x,t)\,\mathrm{d}x - \sum_{i=1}^{N}\big[\theta(x_i) k_i z^2(x_i,t) \\ &\quad + \theta(x_i)\left[\Phi_i - |\psi_i(t)|\right] |z(x_i,t)|\big] \leq 0.\end{aligned} \tag{60}$$

Note indeed that, by (9), the term $\left[\Phi_i - |\psi_i(t)|\right]$ is nonnegative. Therefore, inequality (60) imply that along potential weak solutions of the closed-loop system relation $\dot{V}(t) \leq 0$ holds both beyond and along the discontinuity manifolds $z(x_i,t) = 0$. Thus, $V(t)$ is non-increasing, which means that

$$0 \leq V(t) \leq V(0) \quad \forall t \geq 0. \tag{61}$$

From (61) and (46) and (48), and taking into account that

$$V_1(t) \leq V(t) \leq V(0), \tag{62}$$

$$V_2(t) \leq V(t) \leq V(0), \tag{63}$$

one straightforwardly derives the following uniform upper bounds for $\|z(\cdot,t)\|_{L_2(0,1)}$ and $M_i(t)$

$$\|z(\cdot,t)\|_{L_2(0,1)} \leq \sqrt{2V(0)}, \tag{64}$$

$$M_i(t) \leq \Gamma_i := \Phi_i + \sqrt{\frac{2\gamma_i}{\theta(x_i)} V(0)} \quad \forall i \in \{1, \ldots, N\}. \tag{65}$$

Step 2: Forward completeness of the closed-loop system

The closed-loop trajectories are uniformly bounded in the state space $L_2(0,1)\times\mathbb{R}$ because of the a priori estimate (61) of the Lyapunov function (46) and (48). Hence, along with the Lyapunov function, an arbitrary local solution of the closed-loop system admits an a priori estimate in the state space $L_2(0,1)\times\mathbb{R}$ too. Thus, such a solution is continuously extendible to the right for all $t\geq 0$ because otherwise, its norm would escape to infinity in finite time, which would contradict (61).

Step 3: Uniform boundedness of $\int_0^1\theta(x)z_x^2(x,t)\,\mathrm{d}x$ and $|z(x_i,t)|$

The new Lyapunov candidate function

$$W(t)=\sum_{i=1}^{7}V_i(t) \tag{66}$$

is introduced with

$$V_3(t)=\frac{1}{2}\int_0^1\theta(x)z_x^2(x,t)\,\mathrm{d}x, \tag{67}$$

$$V_4(t)=\sum_{i=1}^{N}\theta(x_i)M_i(t)|z(x_i,t)|, \tag{68}$$

$$V_5(t)=\sum_{i=1}^{N}\left[\theta(x_i)\Phi_i|z(x_i,t)|-\theta(x_i)\psi_i(t)z(x_i,t)\right], \tag{69}$$

and

$$V_6(t)=\sum_{i=1}^{N}\theta(x_i)\frac{\Phi_{\mathrm{d},i}}{\gamma_i}\left(\Gamma_i-M_i(t)\right), \tag{70}$$

$$V_7(t)=\frac{1}{2}\sum_{i=1}^{N}\theta(x_i)\left(\sqrt{k_i}|z(x_i,t)|-\frac{1}{\sqrt{k_i}}\Phi_i\right)^2. \tag{71}$$

The non-negativeness of $V_5(t)$ derives from the inequality

$$|\theta(x_i)\psi_i(t)z(x_i,t)|\leq\theta(x_i)\Phi_i|z(x_i,t)|, \tag{72}$$

whereas the non-negativeness of $V_6(t)$ is due to the previously proven relation (65), namely the existence of the uniform upper bounds Γ_i for the adaptive gains $M_i(t)$.

The time derivatives of the newly introduced functions (67) and (71) along the closed-loop system's solutions are now calculated, starting with $\dot V_3(t)$ for which integration by parts is applied after decomposing the integral similarly to how it was done in (49). This yields

$$\begin{aligned}\dot V_3(t)&=\frac{\mathrm{d}}{\mathrm{d}t}\frac{1}{2}\sum_{i=1}^{N-1}\int_{x_i}^{x_{i+1}}\theta(x)z_{i,x}^2(x,t)\,\mathrm{d}x\\&=\sum_{i=1}^{N-1}\int_{x_i}^{x_{i+1}}\theta(x)z_{i,x}(x,t)z_{i,xt}(x,t)\,\mathrm{d}x\\&=\sum_{i=1}^{N-1}\left[z_{i,t}(x,t)\theta(x)z_{i,x}(x,t)\Big|_{x_i}^{x_{i+1}}-\int_{x_i}^{x_{i+1}}z_{i,t}(x,t)\underbrace{\left[\theta(x)z_{i,x}(x,t)\right]_x}_{z_{i,t}(x,t)}\,\mathrm{d}x\right].\end{aligned} \tag{73, 74}$$

Substituting the PDEs (21) into (74) gives

$$\begin{aligned}\dot V_3(t)=\sum_{i=1}^{N-1}[&z_{i,t}(x_{i+1},t)\theta(x_{i+1})z_{i,x}(x_{i+1},t)\\&-z_{i,t}(x_i,t)\theta(x_i)z_{i,x}(x_i,t)\\&-\|z_{i,t}(\cdot,t)\|^2_{L_2(x_i,x_{i+1})}].\end{aligned} \tag{75}$$

By considering again the norm decomposition

$$\|z_t(\cdot,t)\|^2_{L_2(0,1)}=\sum_{i=1}^{N-1}\|z_{i,t}(\cdot,t)\|^2_{L_2(x_i,x_{i+1})} \tag{76}$$

and exploiting the compatibility conditions (22a) and the time derivative of (28) with (24), one obtains from (75) that

$$\begin{aligned}\dot V_3(t)=-\|z_t(\cdot,t)\|^2_{L_2(0,1)}+\sum_{i=1}^{N-1}[&\underbrace{\theta(x_{i+1})z_t(x_{i+1},t)z_{i,x}(x_{i+1},t)}_{\mu_{i+1}(t)}\\&-\underbrace{\theta(x_i)z_t(x_i,t)z_{i-1,x}(x_i,t)}_{\mu_i(t)}+\theta(x_i)z_t(x_i,t)\left[u_i(t)+\psi_i(t)\right]].\end{aligned} \tag{77}$$

With the definition

$$\mu_i(t):=\theta(x_i)z_t(x_i,t)z_{i-1,x}(x_i,t) \tag{78}$$

and a similar reasoning as that exploited in (31) or (52), it results that

$$\begin{aligned}\dot V_3(t)=&-\|z_t(\cdot,t)\|^2_{L_2(0,1)}-\mu_1(t)+\mu_N(t)\\&+\sum_{i=1}^{N-1}\theta(x_i)z_t(x_i,t)\left[u_i(t)+\psi_i(t)\right]\end{aligned} \tag{79}$$

where, because of (7b) and (23a),

$$\mu_1(t)=\theta(x_1)z_t(x_1,t)z_{0,x}(x_1,t)=0, \tag{80}$$

$$\begin{aligned}\mu_N(t)&=\theta(x_N)z_t(x_N,t)z_{N-1,x}(x_N,t)\\&=\theta(x_N)z_t(x_N,t)\left[u_N(t)+\psi_N(t)\right].\end{aligned} \tag{81}$$

Thus, one gets from (79) with (24), (80), and (81)

$$\dot V_3(t)=-\|z_t(\cdot,t)\|^2_{L_2(0,1)}+\sum_{i=1}^{N}\theta(x_i)z_t(x_i,t)\left[u_i(t)+\psi_i(t)\right]. \tag{82}$$

By inserting control laws (12) into (82) it is obtained that

$$\begin{aligned}\dot V_3(t)=-\|z_t(\cdot,t)\|^2_{L_2(0,1)}+\sum_{i=1}^{N}[&-\theta(x_i)k_iz_t(x_i,t)z(x_i,t)\\&-\theta(x_i)M_i(t)z_t(x_i,t)sign\left(z(x_i,t)\right)+\theta(x_i)z_t(x_i,t)\psi_i(t)].\end{aligned} \tag{83}$$

Evaluating the time derivatives of the remaining functions $V_4(t)$ to $V_7(t)$ yields

$$\begin{aligned}\dot V_4(t)&=\sum_{i=1}^{N}\left[\theta(x_i)\dot M_i(t)|z(x_i,t)|+\theta(x_i)M_i(t)\frac{\mathrm{d}}{\mathrm{d}t}|z(x_i,t)|\right]\\&=\sum_{i=1}^{N}\left[\theta(x_i)\gamma_iz^2(x_i,t)+\theta(x_i)M_i(t)z_t(x_i,t)sign\left(z(x_i,t)\right)\right],\end{aligned} \tag{84}$$

$$\dot{V}_5(t) = \sum_{i=1}^{N} \Big[\theta(x_i)\Phi_i z_t(x_i,t) sign\big(z(x_i,t)\big) - \theta(x_i)\dot{\psi}_i(t) z(x_i,t) - \theta(x_i)\psi_i(t) z_t(x_i,t)\Big], \tag{85}$$

$$\dot{V}_6(t) = \sum_{i=1}^{N} -\theta(x_i)\Phi_{\mathrm{d},i}|z(x_i,t)|, \tag{86}$$

$$\dot{V}_7(t) = \sum_{i=1}^{N} \Big[\theta(x_i) k_i z_t(x_i,t) z(x_i,t) - \theta(x_i)\Phi_i z_t(x_i,t) sign\big(z(x_i,t)\big)\Big]. \tag{87}$$

Note that in the time derivatives $\dot{V}_3(t)$–$\dot{V}_5(t)$ and $\dot{V}_7(t)$ the discontinuous term $sign\big(z(x_i,t)\big)$ appears. Beyond the discontinuity manifolds $z(x_i,t) = 0$ it evaluates to a single value according to (5) and cancels out in the following computation of $\dot{W}(t)$. When sliding $z(x_i,t) = 0$ occurs, the sign-functions are multiplied by the time derivative $z_t(x_i,t)$ which is zero too, thus nullifying the discontinuous term. Hence, the existence of the time derivatives $\dot{V}_3(t)$–$\dot{V}_5(t)$ and $\dot{V}_7(t)$ is possibly violated only at a zero-measure, discrete set of isolated time instants where the solutions $z(x,t)$ cross (rather than slide along) the discontinuity manifolds $z(x_i,t) = 0$. Thus, (83) to (85) and (87) hold true almost always thereby validating all subsequent derivations and stability analyses.

Combining (83) and (87), and reordering, leads to

$$\dot{W}(t) = \sum_{i=1}^{7}\dot{V}_i(t) = -\int_0^1 \theta(x) z_x^2(x,t)\,\mathrm{d}x - \|z_t(\cdot,t)\|^2_{L_2(0,1)} + \sum_{i=1}^{N}\Big[\theta(x_i)\big(\gamma_i - k_i\big)z^2(x_i,t) + \theta(x_i)\big(\psi_i(t) - \dot{\psi}_i(t)\big) z(x_i,t) - \theta(x_i)\big(\Phi_i + \Phi_{\mathrm{d},i}\big)|z(x_i,t)|\Big]. \tag{88}$$

The sign-indefinite term $\theta(x_i)\big(\psi_i(t) - \dot{\psi}_i(t)\big)z(x_i,t)$ in the right-hand side of (88) can be estimated as

$$\Big|\theta(x_i)\big(\psi_i(t) - \dot{\psi}_i(t)\big)z(x_i,t)\Big| \le \theta(x_i)\big(\Phi_i + \Phi_{\mathrm{d},i}\big)|z(x_i,t)| \tag{89}$$

by virtue of (9) and (10). Thus, by virtue of (17) and (89) one can further manipulate the right-hand side of (88) to get

$$\dot{W}(t) \le -\int_0^1 \theta(x) z_x^2(x,t)\,\mathrm{d}x - \|z_t(\cdot,t)\|^2_{L_2(0,1)} \le 0. \tag{90}$$

The latter inequality implies that $W(t)$ is non-increasing, which means that

$$0 \le W(t) \le W(0) \quad \forall t \ge 0. \tag{91}$$

From (91), and taking into account that

$$V_3(t) \le W(t) \le W(0), \tag{92}$$

$$V_7(t) \le W(t) \le W(0), \tag{93}$$

one can derive uniform upper bounds for $\int_0^1 \theta(x) z_x^2(x,t)\,\mathrm{d}x$ and $|z_i(x,t)|$, $i \in \{1,\ldots,N\}$, given by

$$\int_0^1 \theta(x) z_x^2(x,t)\,\mathrm{d}x \le 2W(0), \tag{94}$$

$$|z(x_i,t)| \le \frac{1}{k_i}\Phi_i + \sqrt{\frac{2}{k_i\theta(x_i)}W(0)}. \tag{95}$$

Step 4: Asymptotic state stability

In the last step of the proof, Barbalat's Lemma [30] is employed, after some preliminary manipulations, in order to show asymptotic state stability in the L_2-sense. From (60) it follows that

$$\dot{V}(t) \le -\int_0^1 \theta(x) z_x^2(x,t)\,\mathrm{d}x - \sum_{i=1}^{N}\theta(x_i) k_i z^2(x_i,t). \tag{96}$$

By virtue of Assumption 2, the right-hand side of (96) can be further manipulated as follows

$$\begin{aligned}\dot{V}(t) &\le -\int_0^1 \theta_{\mathrm{m}} z_x^2(x,t)\,\mathrm{d}x - \sum_{i=1}^{N}\theta_{\mathrm{m}} k_i z^2(x_i,t) \\ &= -\theta_{\mathrm{m}}\|z_x(\cdot,t)\|^2_{L_2(0,1)} - \theta_{\mathrm{m}}\sum_{i=1}^{N} k_i z^2(x_i,t).\end{aligned} \tag{97}$$

Rearranging the Poincaré inequality (37) from Lemma 2 and applying it to the function $z(\cdot,t)$ yields

$$\|z_x(\cdot,t)\|^2_{L_2(0,1)} \ge \frac{1}{4}\|z(\cdot,t)\|^2_{L_2(0,1)} - \frac{1}{2}z^2(x_{i^*},t) \tag{98}$$

for an arbitrary $i^* \in \{1,\ldots,N\}$. By considering (98), inequality (97) is further manipulated to

$$\begin{aligned}\dot{V}(t) &\le -\frac{\theta_{\mathrm{m}}}{4}\|z(\cdot,t)\|^2_{L_2(0,1)} + \frac{\theta_{\mathrm{m}}}{2}z^2(x_{i^*},t) - \theta_{\mathrm{m}}\sum_{i=1}^{N} k_i z^2(x_i,t) \\ &= -\frac{\theta_{\mathrm{m}}}{2}V_1(t) - \theta_{\mathrm{m}}\left(k_{i^*} - \frac{1}{2}\right)z^2(x_{i^*},t) - \theta_{\mathrm{m}}\sum_{\substack{i=1\\ i\neq i^*}}^{N} k_i z^2(x_i,t).\end{aligned} \tag{99}$$

By virtue of (18) one obtains that there exists an $i^* \in \{0,\ldots,N\}$ such that $k_{i^*} \ge \frac{1}{2}$, hence,

$$\dot{V}(t) \le -\frac{\theta_{\mathrm{m}}}{2}V_1(t). \tag{100}$$

Integrating both sides of (100) from $t = 0$ to infinity yields

$$\lim_{t\to\infty}\{V(0) - V(t)\} \ge \frac{\theta_{\mathrm{m}}}{2}\int_0^{\infty} V_1(\tau)\,\mathrm{d}\tau. \tag{101}$$

By virtue of (61) if follows that

$$\lim_{t\to\infty}\{V(0) - V(t)\} \in [0, V(0)] \tag{102}$$

which, considered together with (101), shows that the integral term in the right-hand side of (101) exists. To apply Barbalat's Lemma to derive that $V_1(t)$ asymptotically converges to zero, it remains to show that $V_1(t)$ is uniformly continuous. The differentiability of $V_1(t)$ and uniform boundedness of $\dot{V}_1(t)$ are sufficient for this. The expression of $\dot{V}_1(t)$ was previously derived in (58).

By virtue of Assumptions 1 and 2 and (65), (94) and (95) it can be concluded that all terms appearing in the right-hand side of (58) are uniformly bounded, and so $\dot{V}_1(t)$ turns out to be uniformly bounded as well. This implies, according to Barbalat's Lemma, that

$$\lim_{t\to\infty} V_1(t) = \lim_{t\to\infty} \frac{1}{2}\|z(\cdot,t)\|^2_{L_2(0,1)} = 0 \tag{103}$$

which concludes the proof. □

Remark 1. For proving stability it does not suffice to split up the system and consider the subsystems with boundary control individually, as it was already tackled in Reference [26]. The coupling between the subsystems via the compatibility conditions (22a) and (22b) requires a stability proof incorporating all subsystems simultaneously, which represents the major technical challenge addressed in the present work.

Remark 2. It can be verified that not all the actuators are necessary for the stated stability result to be in force, as long as no boundary disturbances are present. In fact, only one actuator placed anywhere in the domain $x \in [0, 1]$ is required. However, additional actuators can be placed at positions where disturbances are expected to occur in order to compensate for their influence.

4 | Simulation Results

The closed-loop behavior of the considered BVP under the proposed control scheme is investigated by numerical simulations of a real-world plant model. The plant under consideration is a metallic beam of length $L = 265$ mm which is insulated along its length and actuated at multiple positions using thermoelectric modules (TEMs). The TEMs exploit the Peltier effect to impose positive or negative heat fluxes at their respective positions. Assuming that the TEMs are narrow compared to the beam length, pointwise actuation can be considered. The positions of the TEMs are given by

$$\xi_1 = 0 \text{ mm}, \quad \xi_2 = 106 \text{ mm}, \quad \xi_3 = 159 \text{ mm}, \quad \xi_4 = L, \tag{104}$$

hence, there are two boundary actuators at the beam ends and two in-domain actuators.

The conversion of electrical current into heat fluxes by the TEMs relies on multiple physical effects. Modelling these effects introduces a degree of uncertainty which prohibits imposing exact heat fluxes as desired by the controller. Hence, matched disturbances are assumed to act at the respective actuation points. In the simulation study these disturbances are set to

$$\begin{aligned} \psi_1(t) &= -10.6\,\text{K} + \varphi(t), & \psi_2(t) &= 14.575\,\text{K} + \varphi(t), \\ \psi_3(t) &= 2.65\,\text{K} + \varphi(t), & \psi_4(t) &= -6.625\,\text{K} + \varphi(t) \end{aligned} \tag{105}$$

where $\varphi(t) = 0.795\,\text{K}\,\sin(0.12\pi t) + 0.53\,\text{K}\,\sin(0.2\pi t)$.

The beam's thermal diffusivity is identified experimentally as $\theta_0 = 8.62 \cdot 10^{-5}\ \frac{\text{m}^2}{\text{s}}$, however, due to material imperfections, it is assumed to vary spatially along the beam length. To incorporate

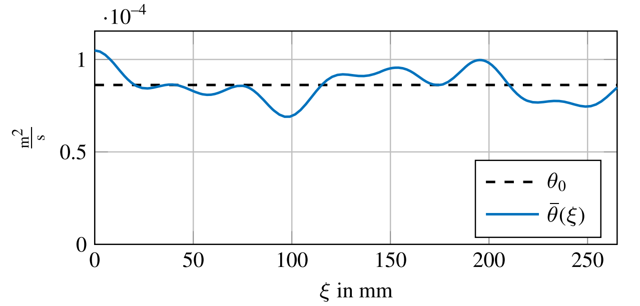

FIGURE 2 | Spatially varying thermal diffusivity $\bar{\theta}(\xi)$ of the metallic beam. The constant θ_0 is experimentally identified whereas the spatial variations are assumed to be caused by material imperfections.

this effect into the model, the identified constant diffusivity θ_0 is adjusted by a spatially varying function to obtain the diffusivity

$$\bar{\theta}(\xi) = \theta_0\left[1 + \frac{1}{10}\cos(12\pi\xi) + \frac{1}{15}\cos(30\pi\xi) + \frac{1}{20}\cos(51\pi\xi)\right] \tag{106}$$

where $\xi \in [0, L]$ is the spatial coordinate. The diffusivity $\bar{\theta}(\xi)$ is depicted in Figure 2.

The control task is to robustly stabilize a desired constant temperature profile $T_r(\xi) = T_r^*$ along the beam despite the presence of the matched disturbances (105). The temperature $T(\xi, t)$ of the beam is modelled by a one-dimensional heat equation. Computing the dynamics of the error variable $\bar{z}(\xi, t) = T(\xi, t) - T_r(\xi)$ and normalization of the spatial domain to $x = \frac{\xi}{L} \in [0, 1]$ leads to the considered BVP (6), (7a) and (7b) with the state $z(x, t) = \bar{z}(Lx, t)$ and the diffusivity function $\theta(x) = \frac{\bar{\theta}(Lx)}{L^2}$. Therefore, the proposed control scheme is applied to the error dynamics with the parameters $k_i = 5.3$ and $\gamma_i = 1.325\ \frac{1}{\text{s}}, \forall i \in \{1, 2, 3, 4\}$. The adaptive gains are initialized as $M_{0,i} = 0$ K, $\forall i \in \{1, 2, 3, 4\}$ whereas the initial temperature of the beam is set to $T(\xi, 0) = 20$ °C. The desired temperature is chosen as $T_r^* = 30$ °C. Note that for the purpose of implementation $sign(0)$ is set to zero.

In order to numerically solve the closed-loop BVP, the semi-discretization approach is followed where the spatial domain $\xi \in [0, L]$ is partitioned into $n = 100$ uniformly spaced solution nodes. The resulting 100th-order finite-dimensional system is then discretized by the forward Euler method with a step size of $T_s = 5 \cdot 10^{-5}$ s.

To better demonstrate the robustness gained from the discontinuous control terms in (12), the proportional parts $-k_i z(x_i, t)$ are activated from the beginning of the simulation whereas the discontinuous parts $-M_i(t)sign\big(z(x_i, t)\big)$ are activated only after $t =$ 6 min. In other words, the adaptive gains are kept at $M_{0,i} = 0$ K in the first part of the simulation, after which the adaptation is activated and $M_i(t)$ adapts according to the proposed adaptation law (13). This way, the influence of the matched disturbances (105) on the closed-loop behavior and the capability of the proposed discontinuous adaptive control to suppress them can be observed more clearly.

The spatiotemporal profile $T(\xi, t)$ of the beam's temperature during the simulation is visualized in Figure 3. It can be seen that starting from the initial temperature, the temperature rises and

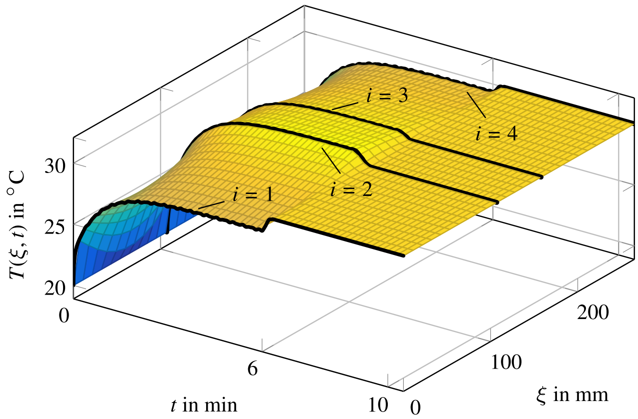

FIGURE 3 | Spatiotemporal profile of the temperature $T(\xi, t)$. The black lines highlight the temperature evolutions at the positions of the four actuators. At $t = 6$ min, the adaptation is activated, leading to a suppression of the disturbances and convergence to the desired temperature profile.

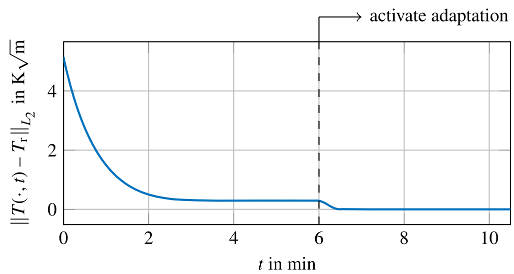

FIGURE 4 | The proportional part of the control law alone is not sufficient to completely reject the matched disturbances, as indicated by the non-vanishing norm $||T(\cdot, t) - T_r||$ in the first part of the simulation. After activating the adaptation, the norm converges towards zero asymptotically.

settles to a profile close to the desired constant temperature T_r^*. However, due to the presence of the matched disturbances, the desired profile $T_r(\xi)$ is not reached exactly, and temperature fluctuations occur, especially visible at the actuator positions ξ_i. After the adaptation is activated at $t = 6$ min, the adaptive gains increase and compensate for the disturbance which leads to convergence towards the desired temperature profile.

Figure 4 displays the time evolution of the norm $\|T(\cdot, t) - T_r\|_{L_2}$, that is, the norm of the difference between the beam's temperature and the desired temperature. It is clearly visible that in the first part of the simulation ($0 \leq t < 6$ min), the norm decreases initially, however, it does not converge towards zero. This indicates that the proportional part of the control law on its own is not sufficient to completely reject the disturbances and stabilize the desired temperature profile. However, after activating the adaptation at $t = 6$ min, the norm starts to decrease again and converges towards zero asymptotically, indicating that the control goal is achieved.

The disturbances (105), together with the adaptive gains $M_i(t)$, are depicted in Figure 5. It can be observed that the adaptive gains individually rise in order to compensate for the disturbances. The graph also highlights a major characteristic of the proposed adaptation laws (13): Since the gains $M_i(t)$ can only increase or remain constant, it may happen that the bounds of the matched disturbances are overestimated, as it is especially visible in the simulation for $i = 3$.

The temperatures at the actuator positions ξ_i are illustrated in Figure 6 and the control signals $u_i(t)$ are shown in Figure 7a. These plots reveal that high-frequency switching of the discontinuous control, that is, a sliding mode along the manifold $z(x_i, t) = 0$, takes place after a finite transient after activating the adaptation. Note that neither the pointwise convergence towards to zero of the state, nor the potential occurrence of sliding modes are, however, predicted by the presented theoretical analysis.

Despite the substantial robustness gained by the discontinuous control, in practical applications chattering phenomena may occur, and, furthermore, the high-frequency switching may significantly reduce the lifetime of the actuators. In fact, the employed TEMs are not designed to switch rapidly between heating and cooling modes. To mitigate these issues, the discontinuous $sign(\cdot)$ function in the control law (12) can be replaced by a continuous approximation, for example, the saturation function $sat(\cdot)$ defined as

$$sat(\sigma) = \begin{cases} \sigma, & |\sigma| \leq 1, \\ sign(\sigma), & |\sigma| > 1 \end{cases}. \tag{107}$$

The same simulation is repeated with the control laws

$$u_i(t) = -k_i z(x_i, t) - M_i(t) sat\left(\frac{1}{\varepsilon} z(x_i, t)\right), \quad i \in \{1, 2, 3, 4\} \tag{108}$$

instead of (12), where ε is a positive constant which determines the width of the linear region of the saturation function. For the simulation a choice of $\varepsilon = 10T_s = 5 \cdot 10^{-4}$ is made. Figure 7b demonstrates that with this modification the control signals $u_i(t)$ become continuous and high-frequency switching is avoided. The overall control performance is similar to the one achieved with the discontinuous control law, as it can be seen in Figure 8 which compares the time evolutions of the norm $\|T(\cdot, t) - T_r\|_{L_2}$ for both cases. A more detailed view of the norm evolution at the second stage of the simulation is provided in Figure 8b, showing that the achieved accuracy is comparable for the two cases.

5 | Summary and Conclusions

An adaptive sliding mode–based control law has been proposed for stabilizing a class of uncertain diffusion processes subject to matched disturbances. The disturbances are assumed to be uniformly bounded along with their time derivatives, whereas the corresponding bounds are unknown. Feedback is applied via a finite number of pointwise actuators located at the boundaries and on the inside of the spatial domain. Measurements of the state are only needed at these locations. The applied control law renders the origin of the closed-loop globally asymptotically stable in the L_2-sense.

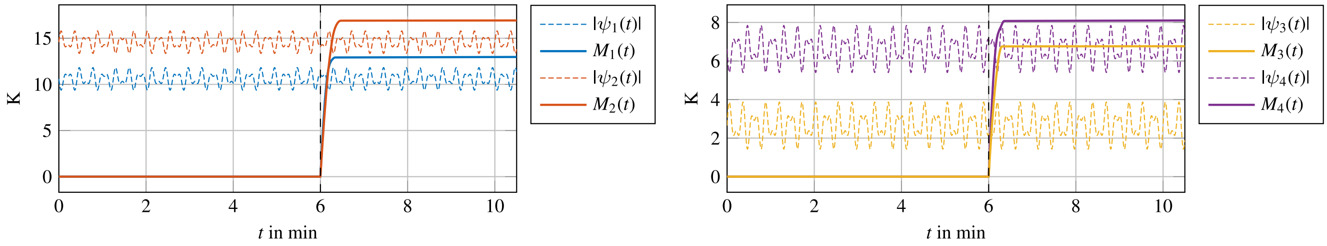

(a) (b)

FIGURE 5 | Magnitude of the matched disturbances $\psi_i(t)$ and the adaptive gains $M_i(t)$. The adaptive gains increase in order to compensate for the disturbances. Since they can only increase or remain constant, overestimation of the disturbance bounds may occur, which is especially visible for $i = 3$. (a) $i \in \{1, 2\}$, (b) $i \in \{3, 4\}$.

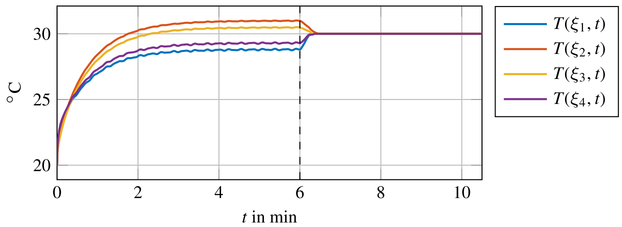

FIGURE 6 | Time evolution of the temperatures at the actuator positions ξ_i. As soon as the adaptation is activated at $t = 6$ min, the discontinuous control terms start rejecting the matched disturbances and the temperatures $T(\xi_i, t)$ reach the desired temperature T_r^*.

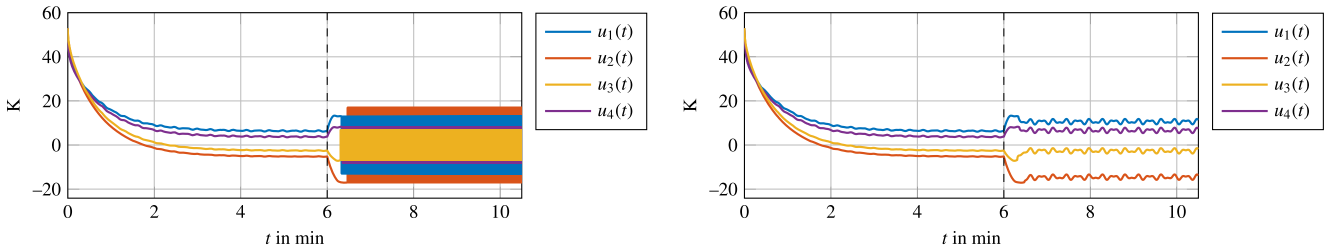

(a) (b)

FIGURE 7 | Control signals $u_i(t)$ employing the *sign*$(\cdot)$ function (left plot) and the *sat*$(\cdot)$ function (right plot). In the former case, high-frequency switching occurs, whereas in the latter case, continuous control signals are achieved. (a) *sign*$(\cdot)$, (b) *sat*$(\cdot)$.

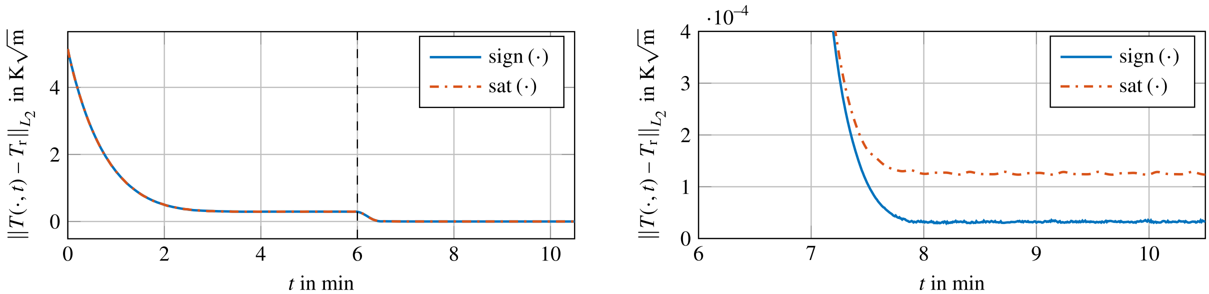

(a) (b)

FIGURE 8 | Comparison of the time evolutions of the norm $\|T(\cdot, t) - T_r\|$ for the discontinuous control law employing the *sign*$(\cdot)$ function and for the continuous approximation using the *sat*$(\cdot)$ function. The continuous control signals are achieved at the cost of a slightly reduced accuracy, as visible in the zoomed view. (a) The whole duration of the simulation, (b) Zoomed view at the second stage of the simulation.

As shown by the presented simulations, the monodirectional nature of the considered gradient-based adaptation can lead to over-estimation of the adaptive gain, which is not desirable as it yields higher chattering in practical applications. Hence, ongoing research is concerned with developing a different kind of adaptation algorithm, which also allows the adaptive gains to decrease.

Another interesting related topic for potential next research is the investigation of the effect of unmatched disturbances acting over the whole spatial domain to demonstrate that ISS-like properties like those shown in Reference [20] are in force in the adaptive setting as well. The experimental validation of the proposed algorithm in laboratory or real-world setups is also an interesting activity to be performed in the future.

Author Contributions

Paul Mayr: investigation, methodology, software, visualization, writing – original draft. **Alessandro Pisano, Stefan Koch, Markus Reichhartinger:** conceptualization, methodology, project administration, writing – original draft.

Acknowledgments

Open Access funding provided by Technische Universitat Graz/KEMÖ.

Conflicts of Interest

The authors declare no conflicts of interest.

Data Availability Statement

Data sharing not applicable to this article as no datasets were generated or analyzed during the current study.

Endnotes

[1] Since the sign-function is later used in the control law, a definition such as $sign(0) = 0$ or a smooth approximation of $sign(\cdot)$ may be mandatory for practical implementation of the control algorithm. Refer to Section 4 for more details.

References

1. Y. Li, M. Vilathgamuwa, T. Farrell, S. S. Choi, N. T. Tran, and J. Teague, "A Physics-Based Distributed-Parameter Equivalent Circuit Model for Lithium-Ion Batteries," *Electrochimica Acta* 299 (2019): 451–469.

2. I. Aksikas, "Optimal Output-Feedback Temperature Regulation of a Catalytic Reverse Flow Reactor PDEs Model," *Journal of Process Control* 103 (2021): 1–7.

3. V. Radisavljevic-Gajic, D. Karagiannis, and Z. Gajic, "The Modeling and Control of (Renewable) Energy Systems by Partial Differential Equations an Overview," *Energies* 16, no. 24 (2023): 8042.

4. M. Krstic and A. Smyshlyaev, *Boundary Control of PDEs: A Course on Backstepping Designs*. Advances in Design and Control, vol. 16 (Society for Industrial and Applied Mathematics, 2008).

5. A. Smyshlyaev and M. Krstic, "Closed-Form Boundary State Feedbacks for a Class of 1-D Partial Integro-Differential Equations," *IEEE Transactions on Automatic Control* 49, no. 12 (2004): 2185–2202.

6. M. Krstic and A. Smyshlyaev, "Backstepping Boundary Control for First Order Hyperbolic PDEs and Application to Systems With Actuator and Sensor Delays," in *2007 46th IEEE Conference on Decision and Control* (IEEE, 2007), 225–230.

7. A. Smyshlyaev and M. Krstic, "Backstepping Boundary Control for PDEs With Non-Constant Diffusivity and Reactivity," in *Proceedings of the 2005, American Control Conference, 2005*, vol. 7 (IEEE, 2005), 4557–4562.

8. S. Wang and F. Woittennek, "Backstepping-Method for Parabolic Systems With In-Domain Actuation," *IFAC Proceedings Volumes* 46, no. 26 (2013): 43–48.

9. A. Smyshlyaev and M. Krstic, *Adaptive Control of Parabolic PDEs* (Princeton University Press, 2010).

10. W. Guo, Z. Hc, and M. Krstic, "Adaptive Error Feedback Regulation Problem for 1D Wave Equation," *International Journal of Robust and Nonlinear Control* 28, no. 15 (2018): 4309–4329.

11. S. Wang, J. Qi, and M. Diagne, "Adaptive Boundary Control of Reaction Diffusion PDEs With Unknown Input Delay," *Automatica* 134 (2021): 109909.

12. S. Wang, M. Diagne, and J. Qi, "Delay-Adaptive Predictor Feedback Control of Reaction Advection Diffusion PDEs With a Delayed Distributed Input," *IEEE Transactions on Automatic Control* 67, no. 7 (2022): 3762–3769.

13. R. Guo, J. Li, K. Sun, T. Wang, and J. Qiu, "Output-Feedback Boundary Adaptive Fault-Tolerant Control for Scalar Hyperbolic Partial Differential Equation Systems With Actuator Faults," *International Journal of Adaptive Control and Signal Processing* 36, no. 11 (2022): 2716–2731.

14. Y. Orlov and V. Utkin, "Sliding-Mode Control in Infinite-Dimensional Systems," *Automatica* 23 (1987): 753–757.

15. Y. Orlov, "Discontinuous Unity Feedback Control of Uncertain Infinite-Dimensional Systems," *IEEE Transactions on Automatic Control* 45 (2000): 834–843.

16. Y. Orlov, *Nonsmooth Lyapunov Analysis in Finite and Infinite Dimensions*. Communications and Control Engineering Series. (Springer, 2022).

17. M. Cheng, V. Radisavljevic, and W.-C. Su, "Sliding Mode Boundary Control of a Parabolic PDE System With Parameter Variations and Boundary Uncertainties," *Automatica* 47 (2011): 381–387.

18. C. Bao, "Sliding Mode Boundary Control for Exponential Stabilization of Linear Parabolic Distributed Parameter Systems Subject to External Disturbance," *International Journal of Robust and Nonlinear Control* 33 (2023): 9364–9390.

19. A. Pisano and Y. Orlov, "Boundary Second-Order Sliding-Mode Control of an Uncertain Heat Process With Unbounded Matched Perturbation," *Automatica* 48, no. 8 (2012): 1768–1775.

20. A. Pisano and Y. Orlov, "On the ISS Properties of a Class of Parabolic DPS With Discontinuous Control Using Sampled-In-Space Sensing and Actuation," *Automatica* 81 (2017): 447–454.

21. J. M. Wang, J. J. Liu, B. Ren, and J. Chen, "Sliding Mode Control to Stabilization of Cascaded Heat PDE ODE Systems Subject to Boundary Control Matched Disturbance," *Automatica* 52, no. 23 (2015): 34.

22. J. Gu and J. Wang, "Sliding Mode Control for N-Coupled Reaction-Diffusion PDEs With Boundary Input Disturbances," *International Journal of Robust and Nonlinear Control* 29, no. 5 (2018): 1437–1461.

23. A. Pilloni, A. Pisano, E. Usai, and Y. Orlov, "Sliding Mode Boundary Control for Heat Equations With Uncertain Dynamic Actuators," in *Proceedings of the IEEE International Workshop Variable Structure System (VSS 2024)* (IEEE, 2024).

24. F. Plestan, Y. Shtessel, V. Brégeault, and A. Poznyak, "New Methodologies for Adaptive Sliding Mode Control," *International Journal of Control* 83 (2010): 1907–1919.

25. S. Roy, S. Baldi, and L. M. Fridman, "On Adaptive Sliding Mode Control Without a Priori Bounded Uncertainty," *Automatica* 111 (2020): 108650.

26. P. Mayr, Y. Orlov, A. Pisano, S. Koch, and M. Reichhartinger, "Adaptive Sliding Mode Boundary Control of a Perturbed Diffusion Process," *International Journal of Robust and Nonlinear Control* 34, no. 15 (2024): 10055–10067.

27. Z. Han, Z. Liu, J. W. Wang, and W. He, "Fault-Tolerant Control for Flexible Structures With Partial Output Constraint," *IEEE Transactions on Automatic Control* 69, no. 4 (2024): 2668–2675.

28. Z. Liu, "Modeling and Adaptive Control for a Spatial Flexible Spacecraft With Unknown Actuator Failures," *Science China Information Sciences* 64 (2021): 1–16.

29. A. Pisano, "Adaptive Unit-Vector Control of an Uncertain Heat Diffusion Process," *Journal of the Franklin Institute* 351, no. 4 (2014): 2062–2075.

30. H. K. Khalil, *Nonlinear Systems*, 3rd ed. (Pearson Education, 2002).